Oncogene (2001) 20, 3845–3856

www.nature.com/onc

Tyrosine kinase inhibitor STI571 enhances thyroid cancer cell motile response to Hepatocyte Growth Factor

Francesco Frasca*[,1,2,3], Paolo Vigneri[2,3,4], Veronica Vella[1], Riccardo Vigneri[1] and Jean YJ Wang*[,2,3]

[1]*Istituto di Medicina Interna, Malattie Endocrine e Del Metabolismo, Università di Catania, Ospedale Garibaldi, Piazza S. Maria di Gesù, 95123 Catania, Italy;* [2]*Division of Biology, University of California, San Diego, 9500 Gilman Drive, La Jolla, California, CA 92093-0322; USA;* [3]*Cancer Center, University of California, San Diego, 9500 Gilman Drive, La Jolla, California, CA 92093-0322; USA;* [4]*Dipartimento di Medicina Sperimentale e Clinica, Università degli Studi di Catanzaro, Magna Graecia, Via T. Campanella 115, 88100 Catanzaro, Italy*

The Hepatocyte Growth Factor (HGF) and its receptor Met are physiological regulators of cell migration. HGF and Met have also been implicated in tumor progression and metastasis. We show here that the tyrosine kinase inhibitor STI571 has a stimulatory effect on HGF-induced migration and branching morphogenesis in thyroid cancer but not in primary or immortalized thyroid epithelial cells. These stimulatory effects of STI571 are observed at a concentration that is clinically relevant. The STI571-enhanced motile response can be correlated with an increase in the Met receptor tyrosine phosphorylation as well as ERK and Akt activation by HGF. Interestingly, one of the targets of STI571, namely the c-Abl tyrosine kinase, is activated by HGF and is recruited at the migrating edge of thyroid cancer cells. These data suggests that c-Abl and/or STI571-inhibited tyrosine kinases can negatively regulate the Met receptor to restrain the motile response in thyroid cancer cells. *Oncogene* (2001) **20,** 3845–3856.

Keywords: Akt; branching morphogenesis; c-Abl; cell motility; ERK; Met; PDGF receptor

Introduction

Cell migration is an important process in embryonic development, tissue remodeling, inflammatory response and wound repair. Cell migration can be regulated by a variety of extracellular factors, including extracellular matrix proteins (ECM), growth factors and chemokines. The ectopic migration of tumor cells during metastasis is a pathological condition that illustrates the importance of controlling the motile capability of cells. A number of physiological activators of the motile response have been identified. These include peptide hormones, their respective receptor tyrosine kinases, intracellular adapter proteins, the small GTPases of the Rho family, phosphatidylinositol 3-kinase (PI3-K), the Extracellular Signal-Regulated Kinase (ERK), Focal Adhesion Kinase (FAK) and the Src tyrosine kinase (Kjoller and Hall, 1999; Parsons and Parsons, 1997; Sieg *et al*., 2000).

An important regulator of cell migration during development is the Hepatocyte Growth Factor (HGF), that binds to and activates the Met receptor tyrosine kinase to stimulate cell motility, morphogenesis and proliferation (Stuart *et al*., 2000). The *hgf* or c-*met* knockout mice die *in utero* and exhibit developmental defects in cell migration (Birchmeier and Gherardi, 1998). Increased expression and/or activity of the Met receptor has been associated with tumor development and possibly tumor metastasis (Jiang *et al*., 1999; Stuart *et al*., 2000). Indeed, overexpression of the Met receptor has been observed in a variety of human tumors, such as lung carcinoma, ovarian cancer, prostate (Stuart *et al*., 2000) and thyroid carcinoma (Di Renzo *et al*., 1995). Furthermore, Met transfected fibroblasts exhibit anchorage-independent growth but are not tumorigenic in nude mice, consistent with a motogenic and invasive phenotype (Giordano *et al*., 1993). *In vitro*, HGF promotes the dismantling of cell-cell adhesion complexes and an epithelial-mesenchymal transition (Stuart *et al*., 2000). In collagen matrix, after HGF stimulation, some cancer cells may form distal branching (Jiang *et al*., 1999).

We have isolated a panel of human thyroid cancer cells that express a high level of the Met receptor and are responsive to the motogenic and morphogenic effect of HGF (Costantino *et al*., manuscript in preparation). We have also derived normal thyroid epithelial cells in primary culture and SV40-LargeT Antigen-immortalized cells expressing a low level of Met receptor. In these cells, we examined the effect of STI571 on HGF-induced motogenic response. STI571 is a 2-phenylaminopyrimidine derivative that can inhibit several tyrosine kinases, including c-Abl, Bcr-Abl, PDGF receptor and the c-Kit receptor tyrosine

*Correspondence: F Frasca, Istituto di Medicina Interna, Malattie Endocrine e del Metabolismo, University of Catania, Piazza S. Maria di Gesu, C/O Ospedale Garibaldi, 95123 Catania, Italy; E-mail: segmeint@mbox.unict.it and JYJ Wang, Division of Biology, University of California, San Diego, 9500 Gilman Drive, Bonner Hall 3317, La Jolla, California, CA 92093-0322, USA;
E-mail: jywang@ucsd.edu
Received 8 December 2000; revised 3 April 2001; accepted 9 April 2001

kinases (Buchdunger *et al*., 1996, 2000; Heinrich *et al*., 2000; Wang *et al*., 2000). In preclinical studies, STI571 has exhibited a specific efficacy in the treatment of chronic myelogenous leukemia (CML) without significant side effects and no apparent toxicity (Druker *et al*., 1996; le Coutre *et al*., 1999). In this study, we have uncovered a previously unknown effect of STI571 in stimulating the cellular response to HGF. We have found that STI571 can increase HGF-induced motility and HGF-induced branching morphogenesis in thyroid cancer cells through an enhancement of the Met receptor signaling.

Results

STI571 increases thyroid cancer cell motility

Previous studies have suggested that HGF (through the Met receptor) activates the PI3-Kinase, ERK and the Src kinase (Stuart *et al*., 2000), which are involved in motility. We therefore examined the effect of inhibitors of PI3-Kinase (LY294002), MEK (PD98059) and Src (PP2) on HGF-induced motility. For comparison, we also tested STI571, which is an inhibitor of several tyrosine kinases including c-Abl, PDGF-R and c-Kit. Figure 1a shows results of a migration assay performed with Ca 18/3, a papillary thyroid carcinoma cell line. In these migration assays, cells were moving across a membrane filter coated on the lower side with collagen and floated above medium with or without HGF (Methods). In the absence of HGF (Figure 1a, left, white bars), LY294002 (number 2) and PP2 (number 4) reduced cell migration by approximately 40% (compare 1 to 2) and 60% (compare 1 to 4) respectively, whereas PD98059 (number 3) was without effect. Surprisingly, STI571 (number 5) increased cell migration by approximately 60% (compare 1 to 5). In the presence of HGF (Figure 1, right, gray bars), migration increased by approximately 50% (number 6). Again, LY294002 (number 7) and PP2 (number 9) inhibited migration, whereas no effect of PD98059 (number 8) was observed on HGF-stimulated migration (compare 6 to 8). Most remarkably, STI571 enhanced HGF-induced migration by approximately 200% (compare 6 to 10). We performed a dose response experiment with STI571 (Figure 1b). Cell migration was increased in a STI571 dose-dependent manner with the maximal stimulation at 1.0 μM. These data suggest that, in thyroid cancer cells, STI571 has an enhancing effect on the basal as well as HGF-induced cell motility (Figure 1a). Moreover, the effect of STI571 occurred within the clinically relevant concentrations (Figure 1b) (Druker *et al*., 1996).

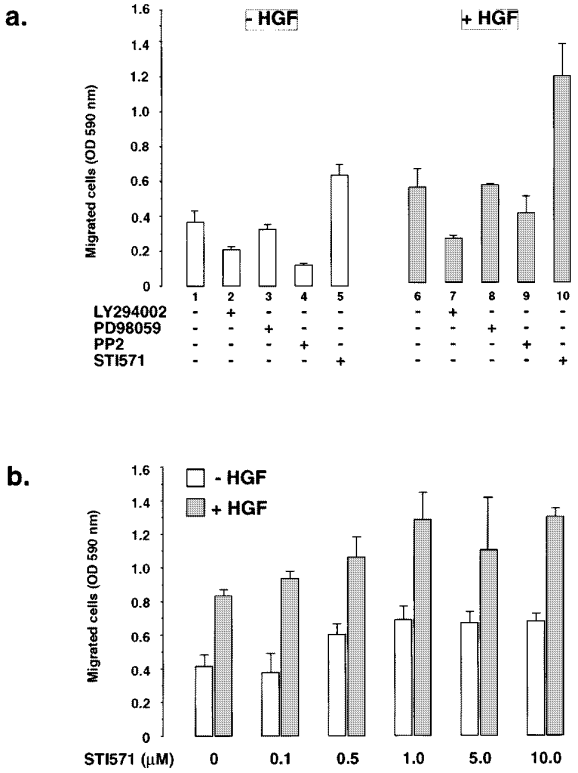

Figure 1 Comparison of different kinase inhibitors on HGF-induced motility. (**a**) The indicated cells were preincubated with STI571 (10 μM), LY294002 (20 μM), PD98059 (50 μM) or PP2 (10 μM) as described in Materials and methods. Cells were then collected and allowed to migrate in lower side collagen-coated transwells for 6 h in the presence or absence of HGF (20 ng/ml) with the continued presence of the indicated inhibitors. White bars: basal migration. Number 1: cells treated with DMSO alone; number 2: cells treated with 20 μM LY294002; number 3: cells treated with 50 μM PD98059; number 4: cells treated with 10 μM PP2; number 5: cells treated with 10 μM STI571. Gray bars: HGF-stimulated migration. Number 6: cells treated with DMSO alone; number 7: cells treated with 20 μM LY294002; number 8: cells treated with 50 μM PD98059; number 9: cells treated with 10 μM PP2; number 10: cells treated with 10 μM STI571. (**b**) Cells were incubated with the indicated concentrations of STI571 as described in Materials and methods. White bars: basal migration. Gray bars: HGF-stimulated migration. Numbers are mean $\pm$ s.d. of three separate experiments performed in triplicate and are calculated as described in Materials and methods

Differential effect of STI571 in cancer versus primary thyroid cells

We examined the effect of STI571 on cell migration in 13 independently derived thyroid cancer cell lines (eight papillary, two follicular and three anaplastic). We also performed migration experiments with two thyroid cell lines, one established by immortalization with the SV40 T-antigen (DR-15) and the other at early passages, in primary culture (N12, see Materials and methods) (Figure 2). In the absence of HGF, STI571 increased migration in nine out of 13 thyroid cancer cell lines (Table 1 and Figure 2) ranging from 30% (CA 301, Table 1, left and Figure 2) up to 140% (BC-PAP, Table 1, left and Figure 2). In the presence of HGF, STI571 significantly enhanced HGF-induced migration in 10 out of 13 cancer cell lines (Table 1 and Figure 2). In ARO and KAK cells, STI571 did not enhance basal

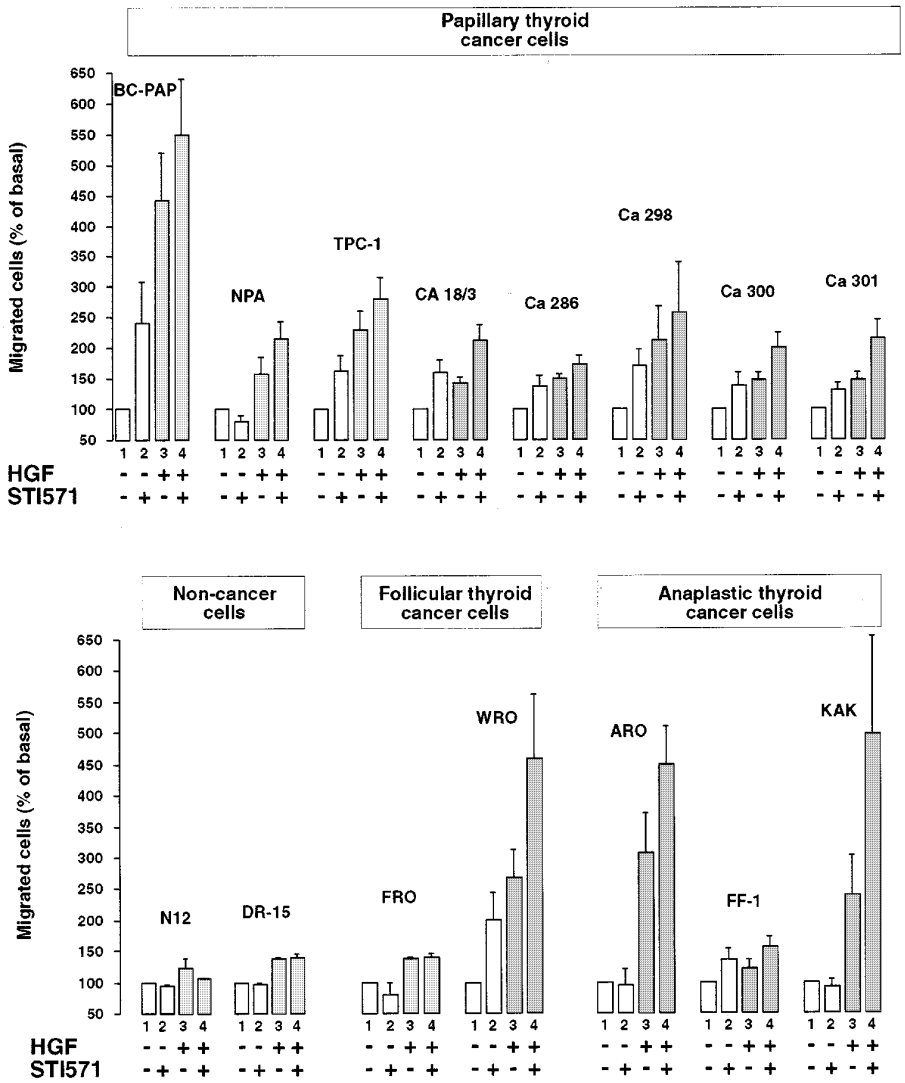

Figure 2 STI571 stimulates HGF-induced motility. The indicated cells were incubated with STI571 (10 μM) for 12 h and then collected and allowed to migrate in lower side collagen-coated transwells for 6 h. Migrated cells were stained with crystalviolet and the absorbance measured at 590 nm. Numbers are expressed as per cent of basal and are mean $\pm$ s.d. of three separate experiments performed in triplicate. Bar 1 (white): cells migrated in serum-free medium; bar 2 (white): cells migrated with 10 μM STI571; bar 3 (gray): cells migrated with 20 ng/ml HGF; bar 4 (gray): cell migrated with HGF and STI571

migration but enhanced HGF-induced migration (Table 1 and Figure 2). By contrast, in cells derived from normal thyroid epithelium (N12 and DR-15) STI571 did not enhance either basal or the HGF-induced motility (Table 1, right and Figure 2), while HGF did, although to a lower level than most cancer cells. These data suggest that STI571 selectively stimulates thyroid cancer cell migration. The Met receptor of these thyroid cancer cells is activated to a low level in the absence of HGF (Costantino *et al*., manuscript in preparation; Bergstrom *et al*., 1999). Therefore, the stimulatory effect of STI571 on thyroid cancer cell migration may be dependent on the increased activity of the Met receptor.

STI571 enhances HGF-induced branching morphogenesis

HGF stimulates branching morphogenesis, which can be demonstrated by seeding cells in a mixture of collagen and proteoglycans (matrigel) (Materials and methods). Without HGF, thyroid cancer cells did not invade the matrigel and formed spheroid structures composed of proliferating cells (Figure 3a, panels A/B). The addition of HGF induced the formation of tubule-like structures indicative of matrigel invasion (Figure 3a, panels C/D). Treatment with STI571 alone caused a small but detectable increase in matrigel invasion (Figure 3a, panels E/F). The combined treatment with HGF and STI571 increased the

Table 1 Migration of neoplastic, immortalized and primary thyroid cells in response to STI571 and HGF

Cell line	*Expression of Met*[a]	*Treatment*	*Migration (% of basal)*	P *value* (t-*test*)[c]	*Cell line*	*Expression of Met*[a]	*Treatment*	*Migration (% of basal)*	P *value* (t-*test*)[c]
Papillary					*Primary*				
BC-PAP	1.7	Basal	100		N12	0.3	Basal	100	
		STI571	239±70	0.0111			STI571	94±3.2	0.023
		HGF	442±77				HGF	124+15	
		HGF+STI571	550+91	0.047			HGF+STI571	106+1	0.0882
					Immortalized				
NPA	2.3	Basal	100		DR-15	0.5	Basal	100	
		STI571	81±8	0.0364			STI571	96±2	0.0223
		HGF	159±26				HGF	140±3	
		HGF+STI571	215±30	0.1835			HGF+STI571	141+4	0.1589
TPC-1	0.5	Basal	100						
		STI571	162±26	0.0054	*Follicular*				
		HGF	231±29		FRO	1.2	Basal	100	
		HGF+STI571	280±35	0.0079			STI571	80±20	0.1366
							HGF	139±3	
Ca 18/3	2.6	Basal	100				HGF+STI571	141±4	0.0931
		STI571	160±21	0.0044					
		HGF	143±8		WRO	0.8	Basal	100	
		HGF+STI571	212±25	0.0071			STI571	198±44	0.0077
							HGF	268±42	
Ca 286	1.4	Basal	100				HGF+STI571	459±103	0.0069
		STI571	138±18	0.0076					
		HGF	151±7						
		HGF+STI571	173±14	0.0079	*Anaplastic*				
					ARO	1.8	Basal	100	
Ca 298	2.8	Basal	100				STI571	93±29	0.6619
		STI571	170±27	0.0199			HGF	307±64	
		HGF	212±55				HGF+STI571	448±63	0.0179
		HGF+STI571	257±83	0.1					
					FF-1	1.3	Basal	100	
Ca 300	1.19	Basal	100				STI571	134±18	0.0221
		STI571	137±23	0.0197			HGF	120±15	
		HGF	149±13				HGF+STI571	157±16	0.0117
		HGF+STI571	200±26	0.0012					
					KAK	1.7	Basal	100	
Ca 301	1.6	Basal	100				STI571	91±14	0.1407
		STI571	130±14	0.0203			HGF	238±63	
		HGF	149±13				HGF+STI571	499±154	0.0023
		HGF+STI571	215±31	0.0135					

[a]Values are the Met-α-Actin ratio obtained by Western blot and densitometric analysis. [b]Number are means±s.d. of three separate experiments performed in triplicate. [c]*P* value is calculated by two tails *t*-test in paired samples

complexity of the branched structures (Figure 3a, panels G/H). The stimulatory effect of STI571 on matrigel invasion was more evident in WRO than in Ca 18/3 cells (Figure 3a). The stimulatory effect of STI571 on HGF-induced morphogenesis was also observed with the Ca 301 cells (not shown). In matrigel cultures we also evaluated the effect of HGF and STI571 on cell proliferation. For this purpose, we seeded cells onto matrigel in 96-well plates and the number of viable cells was evaluated by XTT (Figure 3b) as described in Materials and methods. In both cell lines tested, HGF significantly increased cell number (Figure 3b, compare white to gray bars) indicating that HGF-induced branching morphogenesis is determined by both a change in cell shape and an increase in cell number. Importantly, STI571 did not significantly affect cell proliferation (Figure 3b), suggesting that STI571 influenced the morphogenic rather than the mitogenic effect of HGF.

STI571 enhances Met receptor tyrosine phosphorylation

Previous studies have established STI571 as an inhibitor of the PDGF receptor, the c-Kit receptor and the c-Abl tyrosine kinases at submicromolar concentrations (Druker *et al*., 1996). In order to explain the effect of STI571 on thyroid cancer cells, we examined the expression of PDGF and c-Kit receptors on the WRO cell line, one of the most responsive to STI571 (Table 1, Figure 2). By Western blot, we detected the presence of PDGF-Rβ (190 KDa, Figure 4b, lower panel) whereas we were not able to find any expression of c-Kit (data not shown). Our Western blot data were in accordance with previous findings showing the presence of PDGF-R in thyroid cancer cell lines and the loss of the expression of c-Kit in malignant thyroid cells (Natali *et al*., 1995; Tanaka *et al*., 1995). In WRO cells we therefore examined the effect of different doses of STI571 on the general

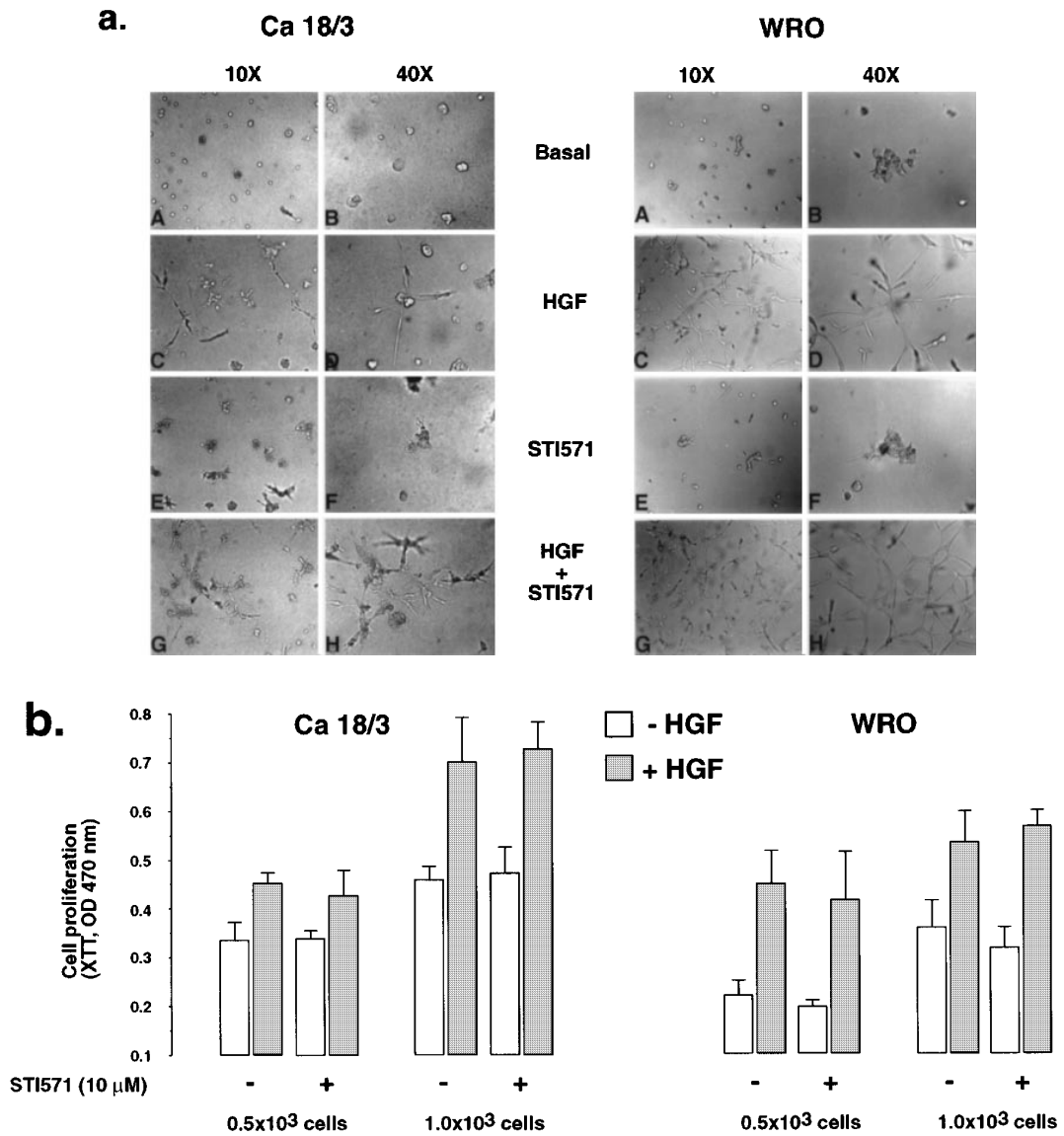

Figure 3 STI571 enhances HGF-induced morphogenesis without affecting cell proliferation. The indicated cells were plated onto matrigel matrix, and then allowed to grow for 5 days under the indicated conditions. (**a**) Panels A/B: serum free medium; panels C/D: plus 20 ng/ml HGF; panels E/F: plus 10 μM STI571; panels G/H: plus HGF and STI571. Cells shown in panels A, C, E, G were scored at 10 × magnification, whereas B, D, F, H were scored at 40 ×. Each figure is representative of three separate experiments performed in triplicate. (**b**). The same cells were plated onto matrigel matrix in 96-multiwell and grown for 5 days in the presence or absence of 10 μM STI571 and stimulated (gray bars) or not (white bars) with 20 ng/ml HGF. After incubation with XTT, plates were read at 470 nm as described in Materials and methods. Numbers are mean ± s.d. of three experiments performed in triplicate

protein tyrosine phosphorylation by anti-Ptyr blot on crude cell lysate (Figure 4a). In serum starved WRO cells, the increasing doses of STI571 caused a detectable albeit slight increase in the tyrosine-phosphorylated proteins (Figure 4a, lanes 1–5). Upon stimulation with PDGF-BB, a significant increase in tyrosine phosphorylation was observed (Figure 4a, compare lane 1 to 11) and, as expected, this increase was inhibited by STI571 (Figure 4a, lanes 11–15). Stimulation with HGF also increased the tyrosine phosphorylation pattern (Figure 4a, compare 1 to 6). Interestingly, the HGF-induced tyrosine phosphorylation was further enhanced by STI571 (Figure 4a, lanes 6–10). We also examined the effect of STI571 on the tyrosine phosphorylation of PDGF-R (Figure 4b) and Met (Figure 4c, d) in WRO cells. In serum starved cells, PDGF-R was not tyrosine phosphorylated (Figure 4b, upper panel, lane 1) and the increasing

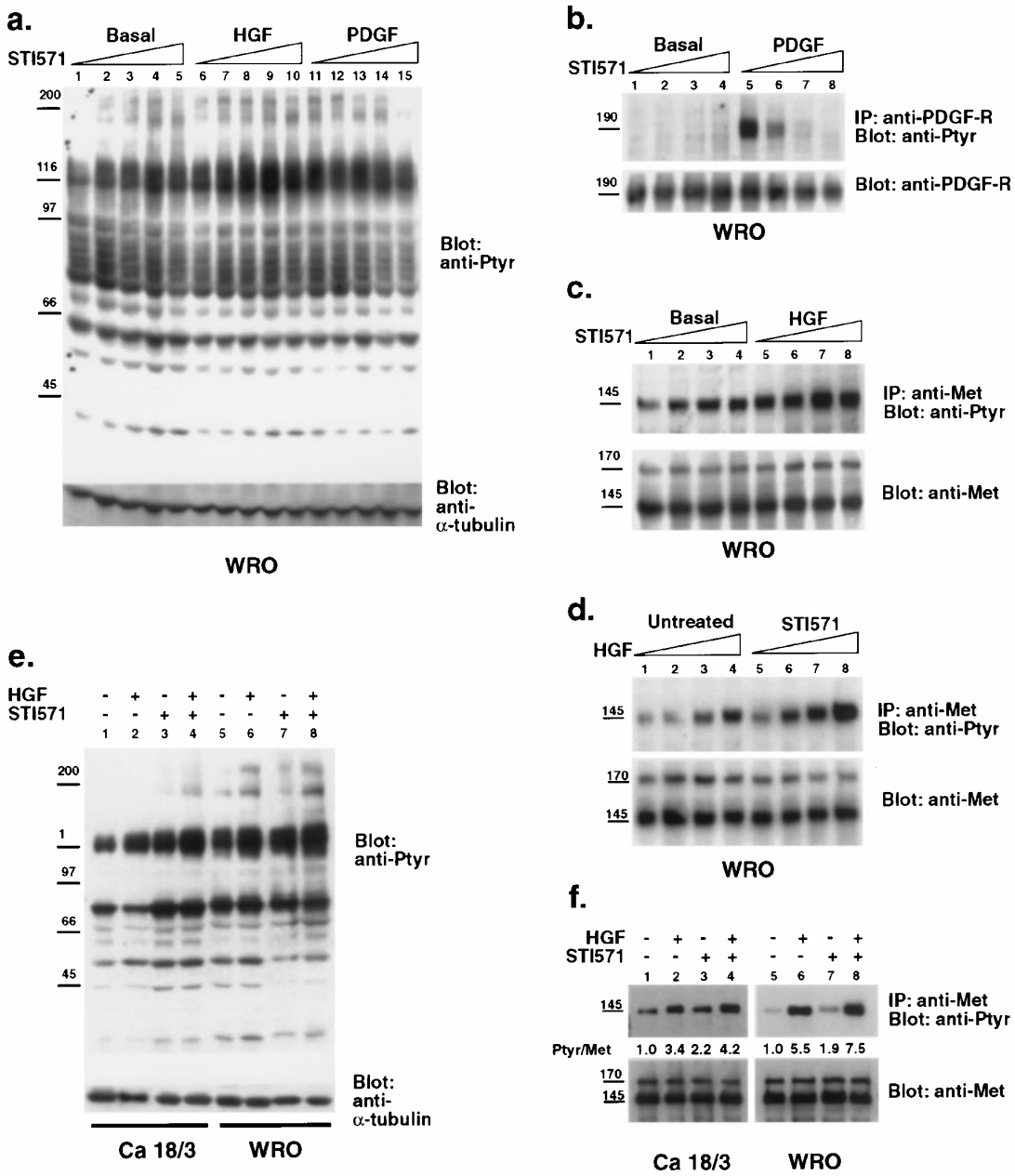

Figure 4 STI571 does not inhibit general tyrosine phosphorylation and enhances Met tyrosine phosphorylation. The indicated cells were serum starved and incubated in the presence or absence of STI571, HGF or PDGF as described in Materials and methods. (**a**) Upper panel: Anti-phosphotyrosine Western blotting on crude lysate in cells incubated in the absence (lanes 1–5) or presence of 20 ng/ml HGF (lanes 6–10) or PDGF (lanes 11–15) and treated with increasing doses of STI571. Lanes 1, 6, 11: untreated cells; lanes 2, 7, 12: 0.1 μM STI571; lanes 3, 8, 13: 0.5 μM STI571; lanes 4, 9, 14: 1.0 μM STI571; lanes 5, 10, 15: 10.0 μM STI571. Lower panel: reblotting with anti-α-tubulin antibody. (**b**) Anti-phosphotyrosine Western blotting on anti-PDGF-R immunoprecipitates (upper lanes) and re-probing with anti-PDGF-R antibody (lower lanes) in cells stimulated (lanes 5–8) or not (lanes 1–4) with 20 ng/ml PDGF and exposed to increasing doses of STI571. Lanes 1 and 5: untreated cells; lanes 2 and 6: 0.1 μM STI571; lanes 3 and 7: 0.5 μM STI571; lanes 4 and 8: 1 μM STI571. (**c**) Anti-phosphotyrosine Western blotting on anti-Met immunoprecipitates (upper lanes) and re-probing with anti-Met antibody (lower lanes) in cells stimulated (lanes 5–8) or not (lanes 1–4) with 20 ng/ml HGF and exposed to increasing doses of STI571. Lanes 1 and 5: untreated cells; lanes 2 and 6: 0.1 μM STI571; lanes 3 and 7: 0.5 μM STI571; lanes 4 and 8: 1 μM STI571. (**d**) Anti-phosphotyrosine Western blotting of anti-Met immunoprecipitates (upper lanes) and re-probing with anti-Met antibody (lower lanes) in cells incubated in the presence (lanes 5–8) or absence (lanes 1–4) of 1 μM STI571 and exposed to increasing doses of HGF. Lanes 1 and 5: unstimulated cells; lanes 2 and 6: 1 ng/ml HGF; lanes 3 and 7: 5 ng/ml HGF; lanes 4 and 8: 20 ng/ml HGF. (**e**) Upper panel anti-phosphotyrosine Western blotting on crude lysate. Lanes 1 and 5: unstimulated cells; lanes 2 and 6: cells stimulated with 20 ng/ml HGF; lanes 3 and 7: cells treated with 10 μM STI571; lanes 4 and 8: cells treated with both HGF and STI571. Lower panel: reblotting with anti-α-tubulin antibody. (**f**) Anti-phosphotyrosine Western

doses of STI571 were without effect on the baseline (Figure 4b, upper panel, lanes 2–4). This result showed that there was not an autocrine PDGF-R stimulation in these cells. When stimulated with 20 ng/ml PDGF-BB, a strong phosphorylation of the receptor was observed that was inhibited by STI571 in a dose-dependent manner (Figure 4b, upper panel, lanes 5–8). Interestingly, a detectable level of Met phosphorylation was observed in serum-starved cells (Figure 4c, upper panel, lane 1), and this was enhanced by the increasing doses of STI571 (Figure 4c, upper panel, lanes 2–4). Most remarkably, HGF-induced tyrosine phosphorylation of Met was also enhanced by STI571 in a dose dependent manner (Figure 4c, upper panels, lanes 5–8). STI571 also increased the phosphorylation response of Met to different doses of HGF (Figure 4d, upper panel, compare lanes 1–4 to 5–8). The same enhancing effect of STI571 on the basal and HGF-induced general protein tyrosine phosphorylation was also observed in Ca 18/3 cells (Figure 4e, compare 1 to 3 and 2 to 4). Again, STI571 increased the Met tyrosine phosphorylation either in the presence or the absence of HGF in Ca 18/3 cells (Figure 4f, compare 1 to 3 and 2 to 4). These data support the idea that the enhancing effect of STI571 on motility and morphogenesis is due to an increase in the tyrosine phosphorylation/activation of the Met receptor. More importantly, the STI571 effect does not appear to be due to a modulation of the PDGF-R as it is not activated under the experimental conditions.

STI571 enhances the activation of ERK and Akt by HGF

Because STI571 increased the tyrosine phosphorylation of the Met receptor tyrosine kinase, we examined whether STI571 could affect the activation (phosphorylation) of ERK1/2 and Akt/PKB in HGF-stimulated cells (Figure 5a,b). In the three thyroid cancer cell lines tested, the phosphorylation of ERK was consistently increased by HGF by 1.5 to twofold (Figure 5a,

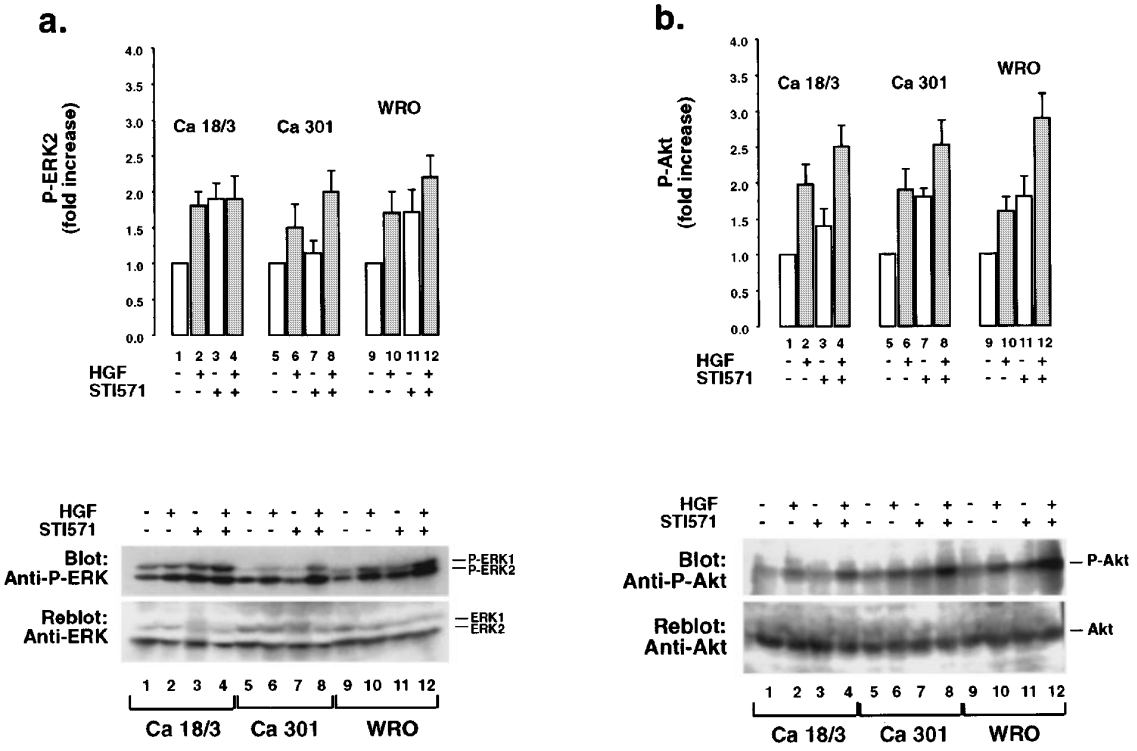

Figure 5 STI571 enhances Met signaling. Phosphorylation of ERK (**a**) and Akt (**b**) in the absence (white bars) or in the presence (gray bars) of HGF in thyroid cancer cells. Lower panels: representative Western blots for Phosho-ERK and Phospho-Akt on crude cell lysate: untreated cells (lanes 1, 5, 9), cells treated with 20 ng/ml HGF (lanes 2, 6, 10), or treated with 10 μM STI571 (lanes 3, 7, 11), or treated with 20 ng/ml HGF and 10 μM STI571 (lanes 4, 8, 12). Upper panels: densitometric analysis (mean$\pm$s.d.) of three separate blots. Numbers have been corrected for total ERK and Akt content

blotting on anti-Met immunoprecipitates (upper lanes) and re-probing with anti-Met antibody (lower lanes). Lanes 1 and 5: unstimulated cells; lanes 2 and 6: cells stimulated with 20 ng/ml HGF; lanes 3 and 7: cells treated with 10 μM STI571; lanes 4 and 8: cells treated with both HGF and STI571. Pictures shown are representative of three separate experiments

compare 1 to 2, 5 to 6 and 9 to 10). Treatment with STI571 alone caused a similar increase in ERK phosphorylation in Ca l8/3 and WRO cells (Figure 5a, compare 1 to 3 and 9 to 11), but the combined effects of HGF and STI571 were not additive. With Ca 301 cells, STI571 did not increase the phosphorylation of ERK but enhanced the effect of HGF on ERK activation. We performed densitometric analysis of the phosphorylation of ERK2 from three independent experiments to establish the reproducibility of these results (Figure 5a, histogram). We also investigated the stimulation of Akt phosphorylation by HGF in the three thyroid cancer cell lines tested (Figure 5b, compare 1 to 2, 5 to 6 and 9 to 10). Again, we observed a stimulatory effect on Akt phosphorylation by treatment with STI571 alone (Figure 5b, compare 1 to 3, 5 to 7 and 9 to 11). The combined treatment of HGF and STI571 further increased Akt phosphorylation in these thyroid cancer cells (Figure 5b, lanes 4, 8, 12). Again, the enhanced activation of Akt by STI571 was reproducibly observed (Figure 5b, histogram). The enhancing effect of STI571 on the HGF-induced activation of ERK and Akt is consistent with its positive effect on HGF-induced cell motility.

c-Abl localizes to the migrating edge of HGF-stimulated cells

Because STI571 affects the activity of the c-Abl tyrosine kinase (Brasher and Van Etten, 2000; Schindler *et al*., 2000), its effect could be in part due to the inhibition of c-Abl. The cytoplasmic c-Abl tyrosine kinase has been implicated in the regulation of cytoskeleton functions associated with cell adhesion, membrane ruffling, neurite outgrowth and axon guidance (Lanier and Gertler, 2000; Lewis *et al*., 1996; Plattner *et al*., 1999). We therefore examined the subcellular localization of c-Abl in the migrating cells. We scraped a monolayer of Ca 18/3 cells to generate a wounded edge and stained these cells with anti-Abl antibody and phalloidin (Figure 6a). In response to the scraping, cells became polarized towards the wound (Nobes and Hall, 1999) (Figure 6a, arrow points to the wound). In the absence of HGF, we detected a diffuse staining of c-Abl with a weak colocalization with F-actin at the leading edge (Figure 6a, panels B/C). After stimulation with HGF, phalloidin-staining showed an increased number of pseudopodia (Figure 6a, panel E), and the c-Abl signal became clearly detectable in these structures (Figure 6a, panel F). After incubation with STI571, phalloidin-staining showed a dramatic epithelial-mesenchymal transition, resulting in spindle-shaped cells with an increased number of pseudopodia and F-actin remodeling (Figure 6a, panel H). In these mesenchymal-like cells, c-Abl colocalized with F-actin in pseudopodia and cytoplasmic protrusions (Figure 6a, panel I). In cells treated with both HGF and STI571, phalloidin-staining showed a further increase in the number of pseudopodia and actin remodeling (Figure 6a, panel K). Again, c-Abl colocalized with F-actin in these cells (Figure 6a, panel L). These results showed that c-Abl was present at the migrating edge of polarized cells.

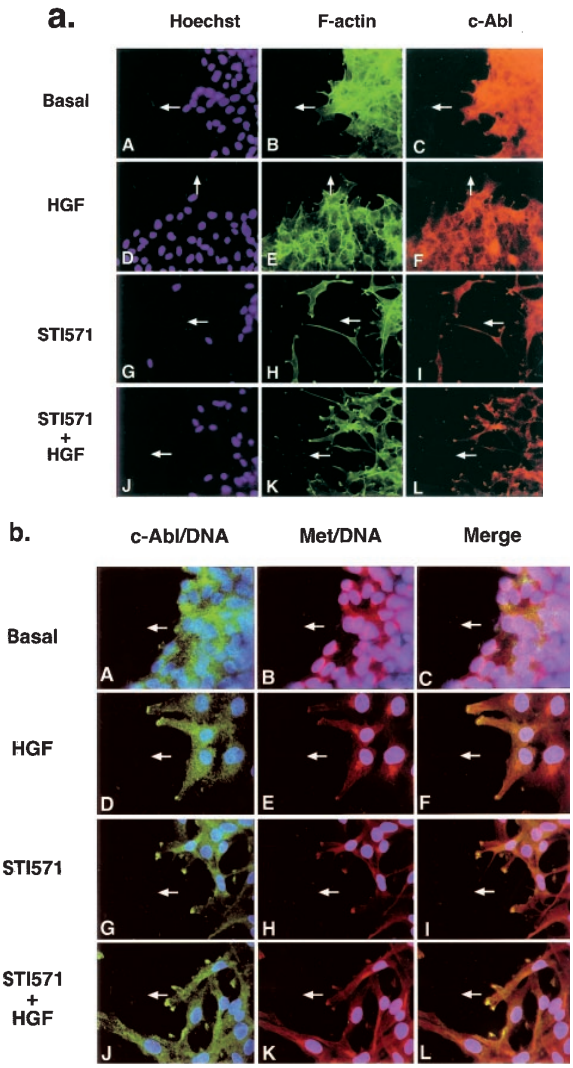

Figure 6 Localization of c-Abl and Met in migrating cells. (**a**) c-Abl immunofluorescence in migrating Ca 18/3 cells stimulated with HGF. Arrows indicate the direction of migrating cells from the edge toward the center of the wound. Panels A, B, C: cells incubated in serum free medium; panels D, E, F: cells incubated with 20 ng/ml HGF; panels G, H, I: cells incubated with 10 μM STI571 alone; panels J, K, L: cells incubated with both HGF and STI571. Panels A, D, G, J show Hoechst-stained cell nuclei; panels B, E, H, K show phalloidin-stained F-actin; panels C, F, I, L 8E9-stained c-Abl. (**b**) Immunofluorescence of Met and c-Abl in migrating Ca18/3 cells stimulated with HGF. Arrows indicate the direction of migrating cells from the edge toward the center of the wound. Panels A, B, C: cells incubated in serum free conditions; panels D, E, F: cells incubated with 20 ng/ml HGF; panels G, H, I: cells incubated with 10 μM STI571; panels J, K, L: cells incubated with both HGF and STI571. Panels A, D, G, J show 8E9-stained c-Abl (green) plus Hoechst stained nuclei (blue); panels B, E, H, K show C-28-stained Met (red) plus Hoechst-stained nuclei (blue); panels C, F, I, L show both c-Abl (green) and Met (red) plus Hoechst-stained nuclei (blue). Representative results from three separate experiments are shown

Met and c-Abl are recruited at the leading edge of migrating cells

We also stained the migrating cells with anti-Met and anti-Abl antibodies and were able to detect a recruitment of c-Abl and Met (Figure 6b) in pseudopodia. In the absence of HGF, anti-Abl (Figure 6b, panel A) and anti-Met (Figure 6b, panel B) each revealed a diffuse pattern (Figure 6b, panel C). After stimulation with HGF, both c-Abl (Figure 6b, panel D) and Met (Figure 6b, panel E) became detectable in pseudopodia. By merging the two signals, it was possible to show that c-Abl and Met were localized in the pseudopodia (Figure 6b, panel F). In the mesenchymal-shaped cells following STI571 treatment, we again detected c-Abl and Met in the pseudopodia (Figure 6b, panel I). The combined treatment with HGF and STI571 increased the number of pseudopodia, in which we continued to observe c-Abl and Met (Figure 6b, panel L). A similar pattern of Met localization was obtained with DL-21 and DO-24 antibodies, recognizing the extracellular domain of the receptor (data not shown). Taken together, these results suggest that the inhibition of c-Abl kinase by STI571 might affect the Met receptor function at the leading edge of the migrating cells and in turn possibly contributing to the enhanced motility.

HGF stimulates c-Abl tyrosine kinase in cells actively spreading onto extracellular matrix

To explore the role of c-Abl in HGF-induced responses, we evaluated the effect of HGF on c-Abl tyrosine kinase activity in Ca 18/3 and WRO cells by an *in vitro* kinase assay as described in Materials and methods. In serum-starved and subconfluent cells, 20 ng/ml HGF did not change c-Abl tyrosine kinase activity (data not shown). Since all the experiments in which we observed the enhancing effect of STI571 were carried out in the presence of extracellular matrix (matrigel, collagen IV), we performed HGF stimulation with Ca 18/3 and WRO allowed to spread onto collagen-coated plates as described in Materials and methods. In these conditions, HGF induced a significant increase in Crk phosphorylation by the c-Abl tyrosine kinase (Figure 7a, upper panels). Densitometric analysis of different experiments, normalized for densitometric values of c-Abl protein (an example is shown in Figure 7a, lower panels), revealed a stimulation in c-Abl tyrosine kinase by HGF by approximately 50% in Ca 18/3 and 25% in WRO cells (Figure 7b). These data suggest that in these cells c-Abl may be involved in the response to HGF to restrain the effect of activated Met.

Discussion

This study shows an enhancement of HGF-induced motility and morphogenesis by the tyrosine kinase inhibitor STI571 in a panel of thyroid cancer cells (Figures 1, 2 and 3). This enhancing effect of STI571 was not observed with inhibitors of PI-3, MEK and the Src tyrosine kinases (Figure 1). In thyroid cancer cells STI571 does not inhibit general protein tyrosine phosphorylation. On the contrary, we found that STI571 can enhance the Met receptor phosphorylation in the absence or the presence of HGF (Figure 4). In STI571-treated cells we also observe an enhanced Akt and ERK activation by HGF (Figure 5). Our data suggests that STI571 may act at an upstream point in the signaling cascade to enhance the Met receptor phosphorylation and thus increasing the signal output to multiple downstream targets, including ERK and Akt. However, we cannot rule out the possibility that STI571 may exert its effect on multiple pathways by inhibiting several different negative regulators.

STI571 is an inhibitor of c-Abl, PDGF receptor and c-Kit tyrosine kinases (Buchdunger *et al*., 2000). C-Kit receptor has been found in normal thyroid epithelial cells, but its expression dramatically decreases in malignant thyroid cells (Natali *et al*., 1995). Consistent with the previous data, we did not detect the c-Kit protein in the WRO cells. Previous report have shown

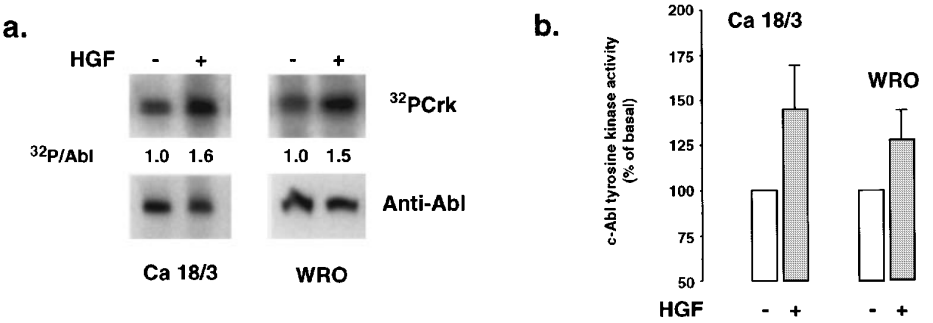

Figure 7 c-Abl tyrosine kinase is stimulated by HGF in cells spreading onto collagen. The indicated cells were allowed to spread onto collagen-coated plates in the presence (gray bars) or absence (white bars) of 20 ng/ml HGF and c-Abl *in vitro* kinase activity toward Crk was performed as described in Materials and methods in anti-Abl immunoprecipitates. (**a**) Upper panels: representative autoradiograms of c-Abl tyrosine kinase *in vitro* assay; lower panels: re-probing with anti-Abl antibody. (**b**). Densitometric analysis (mean ± s.d.) of three separate experiments. Numbers have been normalized for c-Abl content

that thyroid cancer cells express PDGF-R (Heldin *et al*., 1988, 1991) and in fact we detected PDGF-R by Western blot in the WRO cell line (Figure 4b). Importantly, PDGF-R phosphorylation was not detected in serum-starved cells demonstrating that there is not a PDGF-R autocrine loop (Figure 4b). Since all the experiments were performed under serum free conditions, it is unlikely that the STI571 effects could occur via the inhibition of the PDGF-R.

Because STI571 can also inhibit the c-Abl tyrosine kinase, its enhancing effect on HGF-induced response might be due to the inhibition of c-Abl activity. In this regard, the observation that c-Abl tyrosine kinase is activated by HGF and is recruited with the Met receptor at the migrating edge may be relevant (Figures 6 and 7). It is interesting to note that HGF did not stimulate the c-Abl tyrosine kinase in a monolayer of Ca 18/3 or WRO cells. However, HGF activated the c-Abl tyrosine kinase in cells that were engaged to spread onto collagen (Figure 7). Previous work has shown that the c-Abl tyrosine kinase is activated upon cell adhesion to the ECM (Lewis *et al*., 1996). These previous observations together with the present results suggest that HGF might not directly activate the c-Abl tyrosine kinase. Rather, HGF could enhance the adhesion-mediated activation of c-Abl kinase by augmenting the adhesive response to collagen (Trusolino *et al*., 2000). Because cell adhesion to and detachment from the ECM are integral components of cell movement, these results suggest that the c-Abl kinase might function locally at the migrating edge to integrate the HGF and the ECM signals and modulate the motile response.

The effect of STI571 on thyroid cancer cells suggests the existence of mechanisms to restrain Met receptor phosphorylation/activation and cell motility. Remarkably, these STI571-sensitive mechanisms do not appear to be present in normal thyroid cells. This different behavior of cancer and normal thyroid cells could not be correlated with levels of Met receptor expression (Belfiore *et al*., 1997; Di Renzo *et al*., 1995). We observed the enhancing effect of STI571 in thyroid cancer cells TPC-1 and WRO, which expressed the Met receptor at a level comparable to that of normal immortalized cells DR-15 (Figure 2 and Table 1). Another possibility is that the HGF-independent constitutive activity of Met receptor found in thyroid cancer cells (Costantino *et al*., manuscript in preparation; Bergstrom *et al*., 1999, 2000 and Figure 5) may trigger a negative feedback loop to inhibit Met receptor signaling. The existence of these negative pathways may help to explain the apparent paradox in which a better prognosis was associated with a subset of thyroid tumors that overexpress the Met receptor (Belfiore *et al*., 1997). The unraveling of the STI571-sensitive pathways on cell motility may be important for the understanding of thyroid tumor progression and the metastatic potential of thyroid cancer cells.

Because of its ability to inhibit Bcr-Abl, PDGF-R and c-Kit tyrosine kinases, STI571 is being tested in the treatment of chronic myelogenous leukemia (Druker and Lydon, 2000), glioblastoma (Kilic *et al*., 2000) and small cell lung carcinoma (Krystal *et al*., 2000). Our data showing the enhancing effect of STI571 on HGF-induced response suggests that the overall biological effect of STI571 may be dependent upon the expression pattern of tyrosine kinases. Thus, the therapeutic efficacy of STI571 may be highly dependent on which tyrosine kinase pathway is activated in a specific cancer type.

Materials and methods

Reagents and compounds

STI571 has kindly been provided by Novartis (Basel, Switzerland), LY294002, PD98059, PP2 and HGF were purchased from Calbiochem (San Diego, CA, USA); PDGF-BB was purchased from Life Technologies (Rockville, MD, USA). Cell proliferation kit (XTT) was purchased from Roche Diagnostics Corporation (Indianapolis, IN, USA). Matrigel matrix and Anti-Abl monoclonal antibody (Clone 8E9) were purchased from BD PharMingen (San Diego, CA, USA). Anti-Abl (K12) and anti-human Met (C-28) polyclonal antibodies were purchased from Santa Cruz Biotechnology Inc. (Santa Cruz, CA, USA); anti-phosphotyrosine (anti-PTyr) monoclonal antibody 4G10, anti-Met monoclonal antibodies (clone DL-21 and DO 24), anti-PDGF-R A/B polyclonal antibody, anti-c-Kit rabbit antiserum from Upstate Biotechnology, Inc. (Waltham, MA, USA); anti-Phospho p42/44 MAP Kinase (Thr202/Tyr204), anti-MAP kinase, anti-Phospho Akt (Ser473) and anti-Akt polyclonal antibodies from Cell Signaling Tec. (Beverly, MA, USA). Protein A/G Sepharose was purchased from Pharmacia (Uppsala, Sweden). All the other reagents described were purchased from Fisher Scientific (Houston, TX, USA).

Cells

The papillary thyroid cancer cell lines Ca 18/3, Ca 286, Ca 298, Ca 300, Ca 301 and the anaplastic thyroid cancer cell line FF-1 were established in our laboratory from primary cultures. Normal thyroid cells in primary culture were prepared by dissociation of fresh normal thyroid tissue, collected at surgery, with collagenase IV (1 mg/ml in PBS at 37°C in continuous rotation). DR-15 cell line was derived from normal thyroid cells by immortalization with SV-40 Large-T antigen. The papillary thyroid cancer cell lines BC-PAP, TPC-1, NPA, the follicular thyroid cancer cell lines WRO, FRO and the anaplastic thyroid carcinoma cell lines ARO, KAK were kindly provided by Dr A Fusco (Catanzaro, Italy). The expression degree of the Met receptor protein in these cell lines was assessed by densitometric analysis in anti-Met Western blot performed on crude cell lysate. To normalize Met expression levels, the same filters were re-probed with an anti-α-actin antibody (Sigma, St. Louis, MO, USA). All lines were grown in RPMI (Irvine Scientific, Santa Ana, CA, USA) or (in the case of DR-15) DMEM plus 10% FBS (Omega Scientific, Tarzana, CA, USA).

Migration assay

Migration assay was performed as previously described (Sieg *et al*., 1998) with the following modifications. Subconfluent thyroid cancer cells were preincubated with STI571 (0.1, 0.5,

1.0, 5.0 and 10 μM for 12 h) or with LY294002 (20 μM), PD98059 (50 μM) and PP2 (5 μM) for 1 h. Following pre-incubation, cells were then detached with PBS + 5 mM EDTA, resuspended at 10^6/ml. 10^5 cells, in serum free medium, and placed on 6.5 mm diameter polycarbonate filters (8 μM pore size, Costar, from Fisher Scientific), coated at the lower side with 250 μg/ml collagen IV. Then filters were placed over bottom chambers containing 500 μl of serum-free medium (RPMI or DMEM, depending on cell type) with or without HGF (20 ng/ml), STI571 (0.1, 0.5, 1.0, 5.0 and 10 μM), LY294002 (20 μM), PD98059 (50 μM), PP2 (5 μM) and incubated for 6 h at 37° with 5% CO_2. At the end of 6 h, cells on the upper surface of the filters were removed with a cotton swab and the filters stained with crystal violet solution (0.05% crystal violet in PBS + 20% ethanol). Filters were then placed in 24 multiwell plates containing 250 μl/well of 10% acetic acid and incubated for 30 min at room temperature under agitation to elute the dye. Samples were then measured at 590 nm. Row numbers obtained were reported as per cent of basal. Cell migration in these experiments is critically dependent on the coating of the filters with the appropriate matrix protein.

Preparation of cell lysate and Western blot

Subconfluent cells were incubated with 0.1, 0.5, 1.0, 10 μM STI571 in serum free medium for 12 h, stimulated with HGF for 10 min (1.0, 5.0 and 20 ng/ml) or PDGF-BB (20 ng/ml). Cells were washed twice with PBS (pH 7.4) and lysed in RIPA buffer (150 mM NaCl, 1% Nonidet P-40, 50 mM Tris [pH 7.4], 10 mM sodium pyrophosphate, 100 mM NaF, 2 mM PMSF, 2 mM sodium vanadate, 10 μg/ml pepstatin, 10 μg/ml aprotinin, 10 μg/ml leupeptin). After being scraped, the samples were rotated for 15 min at 4°C. Insoluble material was separated from soluble extract by microcentrifugation at 10 000 *g* for 10 min at 4°C. The protein concentration was determined by the Bradford assay (BioRad, Hercules CA, USA). For immunoprecipitation 0.5–1 mg proteins were incubated with 4 μg of the indicated antibodies and protein A/G sepharose. For Western blot on crude cell lysate, after addition of 5 × samples buffer, samples (50 μg protein) were heated at 95°C for 10 min. Immunoblottings were performed using 1 μg/ml of the indicated antibodies. All immunoblots were revealed by enhanced chemiluminescence (Amersham, Little Chalfont, UK), autoradiographed, and subjected to densitometric analysis. Densitometric results have been corrected for the total protein content.

Matrigel assay

Cells were collected and plated in a 48-multiwell (5×10^3 cells/well in 300 μl) previously coated with 300 μl of matrigel (BD Transduction Laboratories, San Diego, CA, USA). After 2 h, complete medium was replaced with serum free medium. Cells were allowed to grow and form tubule like-structures for 5 days in the presence or absence of STI571 (1 and 10 μM) and HGF (20 ng/ml). The medium and the stimulators were replaced every 2 days. The cells were scored with an inverted microscope at 10 × and 40 × magnification and photographed. To evaluate proliferation in matrigel, cells were plated in triplicate on a 96-multiwell (0.5 and 1.0×10^3 cells/well in 100 μl) previously coated with 100 μl of matrigel. After 2 h, complete medium was replaced with serum free medium. Cells were allowed to grow for 5 days in the absence or presence of STI571 and HGF. Then, 50 μl of XTT solution (Roche Diagnostics Corporation, Indianapolis, IN, USA) was added and plates incubated for 4 h at 37°C in the incubator. Absorbance was read at 470 nm, according to the manufacturer's instructions.

c-Abl in vitro *kinase*

Subconfluent cells were serum starved for 24 h. Cells were then detached by PBS + 5 mM EDTA, resuspended in serum free medium, and kept in suspension for 1 h at 37°C. After cells were allowed to attach onto collagen IV-coated (0.25 mg/ml) (Sigma, St. Louis, MI, USA) 100 mm Petri dishes in the presence/absence of HGF (20 ng/ml) for 30 min. After lysis and immunoprecipitation with anti-c-Abl polyclonal antibody (K12), samples were incubated for 40 min with 20 μl of a kinase mixture containing 1 μg GST-Crk, 10 μM ATP, 10 μCi $^{32}\gamma$-P-ATP (ICN, Costa Mesa, CA, USA) in Tris 10 mM [pH 7.4], 10 mM $MgCl_2$, 1 mM DTT. The reaction was then stopped with Laemli buffer, and samples were boiled for 10 min. After SDS–PAGE, filters containing c-Abl and phosphorylated Crk were autoradiographed and then probed with anti-Abl antibody. C-Abl tyrosine kinase activity was quantitated by densitometric analysis of phosphorylated Crk, and normalized for the densitometric results obtained from anti c-Abl Western blot.

Indirect immunofluorescence

For studies in migrating cells under HGF stimulation, cells were grown on coverslips until confluent. These monolayers were wounded with a pipet tip and incubated in the presence/absence of HGF (20 ng/ml) and STI571 (10 μM) in serum free medium for 6 h (Nobes and Hall, 1999). Cells were fixed with 3.7% formaldehyde for 20 min, washed once with PBS and then permeabilized for 10 min with 0.3% Triton X-100. Cells were blocked at room temperature for 1 h with 10% Normal Goat Serum and then incubated with monoclonal anti-Abl 8E9 antibody (30 μg/mL) or anti-Met (C-28) polyclonal antibody (5 μg/ml), or anti-Met monoclonal antibodies (DL-21, DO24) for 2 h. The cover slips were washed with PBS and incubated 1 h with goat anti-mouse or anti-rabbit secondary antibody Alexa Fluor 594, 488 (Molecular Probes, Eugene, OR, USA) or, in the case of c-Abl/F-actin double staining, with Phalloidin-conjugated Alexa Fluor 488 (Molecular Probes). Cells were then washed again with PBS and stained with Hoechst 33258 (Sigma, St. Louis, MO, USA) to visualize the nuclei. After further washing, cover slips were mounted onto glass slides with gel mount (Biomeda, Foster City, CA, USA) and stored at 4°C for 12 h in the dark. Epifluorescence microscopy was performed with a Nikon microscope and two-dimensional images were digitally acquired with a 0.60 × HRD060-NIK CCD-Camera (Diagnostic Instruments, Sterling Heights, MI, USA) using a 60 × 1.40 oil objective. Images were merged using Image Pro Plus Software (Media Cybernetics, Silver Spring, MD, USA).

Statistical analysis

Migration experiments and Phosho-ERK/Akt results in response to HGF and STI571 were compared by two-way analysis of variance. Statistical analysis was carried out with Microsoft Excel software.

Acknowledgments
We thank Novartis for STI571. F Frasca is a recipient of a fellowship from Fondazione Italiana Ricerca sul Cancro

(FIRC, Italy). These studies were supported by grants from the National Institute of Health (USA) to JYJ Wang (HL57900), and from Associazione Italiana Ricerca sul Cancro (AIRC) and Ministero dell'Universita' e della Ricerca Scientifica e Tecnologica (MURST, Italy) to R Vigneri.

References

Belfiore A, Gangemi P, Costantino A, Russo G, Santonocito GM, Ippolito O, Di Renzo MF, Comoglio P, Fiumara A and Vigneri R. (1997). *J. Clin. Endocrinol. Metab.,* **82,** 2322–2328.

Bergstrom JD, Hermansson A, Diaz de Stahl T and Heldin NE. (1999). *Br. J. Cancer.,* **80,** 650–656.

Bergstrom JD, Westermark B and Heldin NE. (2000). *Exp. Cell Res.,* **259,** 293–299.

Birchmeier C and Gherardi E. (1998). *Trends Cell. Biol.,* **8,** 404–410.

Brasher BB and Van Etten RA. (2000). *J. Biol. Chem.,* **29,** 35631–35637.

Buchdunger E, Cioffi CL, Law N, Stover D, Ohno-Jones S, Druker BJ and Lydon NB. (2000). *J. Pharmacol. Exp. Ther.,* **295,** 139–145.

Buchdunger E, Zimmermann J, Mett H, Meyer T, Muller M, Druker BJ and Lydon NB. (1996). *Cancer Res.,* **56,** 100–104.

Di Renzo MF, Olivero M, Serini G, Orlandi F, Pilotti S, Belfiore A, Costantino A, Vigneri R, Angeli A and Pierotti MA. *et al.* (1995). *J. Endocrinol. Invest.,* **18,** 134–139.

Druker BJ and Lydon NB. (2000). *J Clin Invest.,* **105,** 3–7. Review.

Druker BJ, Tamura S, Buchdunger E, Ohno S, Segal GM, Fanning S, Zimmermann J and Lydon NB. (1996). *Nat. Med.,* **2,** 561–566.

Giordano S, Zhen Z, Medico E, Gaudino G, Galimi F and Comoglio PM. (1993). *Proc. Natl. Acad. Sci. USA,* **90,** 649–653.

Heinrich MC, Griffith DJ, Druker BJ, Wait CL, Ott KA and Zigler AJ. (2000). *Blood,* **96,** 925–932.

Heldin NE, Cvejic D, Smeds S and Westermark B. (1991). *Endocrinology,* **129,** 2187–2193.

Heldin NE, Gustavsson B, Claesson-Welsh L, Hammacher A, Mark J, Heldin CH and Westermark B. (1988). *Proc. Natl. Acad. Sci. USA,* **85,** 9302–9306.

Jiang W, Hiscox S, Matsumoto K and Nakamura T. (1999). *Crit. Rev. Oncol. Hematol.,* **29,** 209–248.

Kilic T, Alberta JA, Zdunek PR, Acar M, Iannarelli P, O'Reilly T, Buchdunger E, Black PM and Stiles CD. (2000). *Cancer Res.,* **60,** 5143–5150.

Kjoller L and Hall A. (1999). *Exp. Cell Res.,* **253,** 166–179.

Krystal GW, Honsawek S, Litz J and Buchdunger E. (2000). *Clin. Cancer Res.,* **6,** 3319–3326.

Lanier LM and Gertler FB. (2000). *Curr. Opin. Neurobiol.,* **10,** 80–87.

le Coutre P, Mologni L, Cleris L, Marchesi E, Buchdunger E, Giardini R, Formelli F and Gambacorti-Passerini C. (1999). *J. Natl. Cancer Inst.,* **91,** 163–168.

Lewis JM, Baskaran R, Taagepera S, Schwartz MA and Wang JY. (1996). *Proc. Natl. Acad. Sci. USA,* **93,** 15174–15179.

Natali PG, Berlingieri MT, Nicotra MR, Fusco A, Santoro E, Bigotti A and Vecchio G. (1995). *Cancer Res.,* **55,** 1787–1791.

Nobes CD and Hall A. (1999). *J. Cell. Biol.,* **144,** 1235–1244.

Parsons JT and Parsons SJ. (1997). *Curr. Opin. Cell. Biol.,* **9,** 187–192.

Plattner R, Kadlec L, DeMali KA, Kazlauskas A and Pendergast AM. (1999). *Genes Dev.,* **13,** 2400–2411.

Schindler T, Bornmann W, Pellicena P, Miller WT, Clarkson B and Kuriyan J. (2000). *Science,* **289,** 1938–1942.

Sieg DJ, Hauck CR, Ilic D, Klingbeil CK, Schaefer E, Damsky CH and Schlaepfer DD. (2000). *Nat. Cell. Biol.,* **2,** 249–256.

Sieg DJ, Ilic D, Jones KC, Damsky CH, Hunter T and Schlaepfer DD. (1998). *EMBO J.,* **17,** 5933–5947.

Stuart KA, Riordan SM, Lidder S, Crostella L, Williams R and Skouteris GG. (2000). *Int. J. Exp. Pathol.,* **81,** 17–30.

Tanaka T, Umeki K, Yamamoto I, Kotani T, Sakamoto F, Noguchi S and Ohtaki S. (1995). *Endocr. J.,* **42,** 723–728.

Trusolino L, Cavassa S, Angelini P, Ando M, Bertotti A, Comoglio PM and Boccaccio C. (2000). *FASEB J.,* **14,** 1629–1640.

Wang WL, Healy ME, Sattler M, Verma S, Lin J, Maulik G, Stiles CD, Griffin JD, Johnson BE and Salgia R. (2000). *Oncogene,* **19,** 3521–3528.